JOURNAL OF SOLID STATE CHEMISTRY 117, 261–268 (1995)

Electrical and Magnetic Properties of $LaMo_{8-x}O_{14}$ Containing Isolated Mo_8 Clusters

K. V. Ramanujachary,[1] E. Berry Jones, and M. Greenblatt[2]

Department of Chemistry, Rutgers University—The State University of New Jersey, Piscataway, New Jersey 08855-0939

and

W. H. McCarroll

Chemistry Department, Rider College, Lawrenceville, New Jersey 08648-3099

Received November 21, 1994; accepted November 21, 1994

Single crystal specimens of $LaMo_{8-x}O_{14}$ ($x = 0$ and 0.3) suitable for transport property measurements have been prepared by electrolyzing fused mixtures of sodium and rare earth molybdates. Electrical resistivity measurements with the current parallel to the *ab* plane of $LaMo_{8-x}O_{14}$ containing the quasi-discrete units of Mo_8 clusters showed semiconducting behavior down to 20 K for both compounds. The electrical resistivity in the *ab* plane ($\rho_{ab}^{300K} = 5 \times 10^{-3}$ ohm · cm) of $LaMo_{7.70}O_{14}$ is an order of magnitude smaller than the corresponding value for the fully stoichiometric compound ($\rho_{ab}^{300K} = 4.4 \times 10^{-2}$ ohm · cm). Furthermore, the ρ_{ab}^{300K} of $LaMo_{7.70}O_{14}$ is a factor of 4 lower than that measured along the *c*-axis ($\rho_c^{300K} = 2 \times 10^{-2}$ ohm · cm) implying quasi-low-dimensional behavior. The thermal activation energy for electrical conductivity estimated from the $\ln\rho$ vs $1000/T$ plots showed a significant decrease near ~70 K and 130 K for $LaMo_{7.70}O_{14}$ and $LaMo_8O_{14}$, respectively. The magnetic susceptibility data collected on a batch of randomly oriented crystals revealed the presence of local moments in $LaMo_{7.7}O_{14}$, while the stoichiometric analogue was diamagnetic. The semiconducting nature of the $LaMo_{8-x}O_{14}$ phases may be attributed to the unfavorable intercluster distance (3.08 Å) as well as positional and configurational disorder of the Mo_8 clusters.

INTRODUCTION

Metal atom clusters in the form of bifaced capped octahedra are quite rare and, until recently, were confined exclusively to organometallic molecular systems. The first example of such M_8 clusters in oxide systems was found for $LaMo_{7.70}O_{14}$ and in the isotypic but stoichiometric $NdMo_8O_{14}$ (1, 2). In both of these compounds the clusters are found in the form of the so-called *cis* edge-sharing type shown in Fig. 1(a). Interestingly, this particular isomeric form, hereafter referred to simply as the *cis* form, had not been seen before in chemical systems. The only difference between the lanthanum and neodymium compounds is that the face capping sites are only 85% occupied in the former.

The clusters are arranged in layers parallel to the *ab* plane of the orthorhombic unit cell, as shown in Fig. 2 (2). Within these distorted clusters the metal–metal distances range from approximately 2.6 to 2.8 Å. An Mo–Mo distance of about 3.08 Å is also observed between clusters. Although this intercluster distance is too long to be considered a metal–metal bond, such interactions could influence electronic properties. Between the layers, along the orthorhombic *c* axis, the Mo–Mo distances are approximately 3.6 Å. Further, Mo–O distances are on the average slightly shorter within the layers than between them, suggesting the possibility of quasi-low-dimensional electronic behavior.

Subsequently Leligny, *et al.* reported the existence of a fully stoichiometric form of $LaMo_8O_{14}$ which could best be described in terms of a modulated structure (3) with the modulation wave vector q^* having the components $\langle 0, 1/3, 0\rangle$. Here the Mo_8 containing layers consist of both *cis* and *trans* (Fig. 1(c)) clusters with an average probability of approximately 65 and 35%, respectively. In fact, the actual probability distribution of the two forms is a function of the modulation along *b*. Further, the *cis* and *trans* forms may adopt two different configurations within the lattice. The modulation appears to arise from the disordering of lanthanum atoms onto two different sites (with different occupancies), which would result in abnormally close La–Mo distances were it not for the modulation.

[1] Present Address: Rowan College, Glassboro, New Jersey 08028-1701.

[2] To whom correspondence should be addressed.

0022-4596/95 $12.00

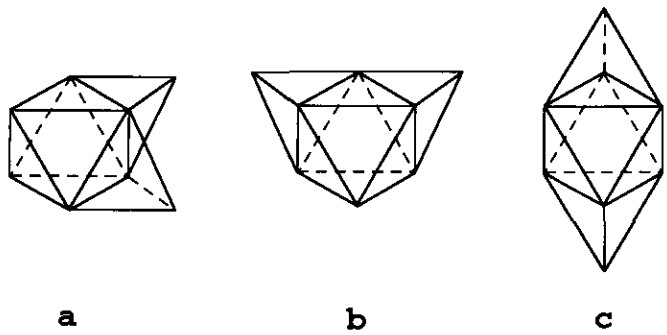

FIG. 1. The isomeric forms of bifaced capped octahedra.

Very recently Kerihuel and Gougeon discovered a third form for $LnMo_8O_{14}$ type phases, where rare earth may be cerium (4) or lanthanum (5). Here, the *b* axis is doubled and ordered, and alternate layers of *cis* and *trans* clusters are found. These phases are prepared in pure form by a solid state reaction at 1800–2100 K, while modulated $LaMo_8O_{14}$ and $LaMo_{7.70}O_{14}$ are prepared by fused salt electrolysis.

A common feature in all of these compounds is an Mo–O network derived from Mo_8O_{24} units (Fig. 3) formed by capping Mo_6O_{18} clusters which share edges and corners to form Mo_8O_{20} slabs in the *ab* plane. These slabs then share outer corners along the *c* direction to complete the 3-dimensional network (1). The oxygens are in a very nearly close-packing arrangement. Of the 64-close-packed sites per unit cell, 56 are occupied by oxygen, 4 by La, and 4, representing the center of the clusters, are vacant.

Despite the existence of such a rich structural variety of ternary molybdenum oxides containing metal–metal bonded clusters, few studies are reported in the literature of their physical properties, in particular their electrical

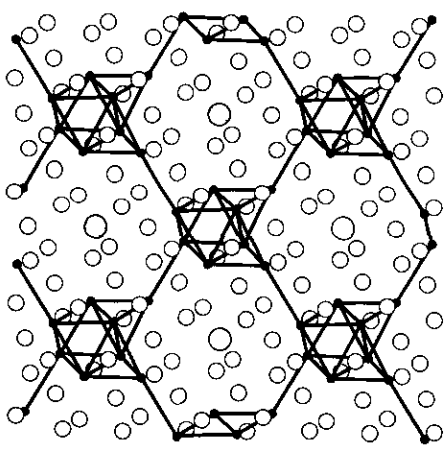

FIG. 2. Layer of $LaMo_{7.70}O_{14}$ structure showing Mo cluster bonds and intercluster linkages. Medium and large circles are O and La respectively. [001] projection

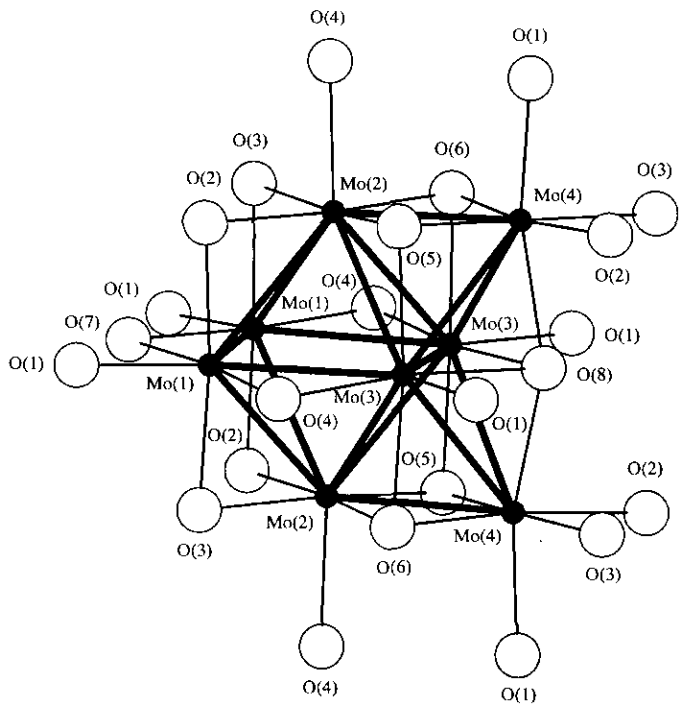

FIG. 3. The *cis*-bifaced capped Mo_8 cluster fragment with its oxygen environment.

and magnetic properties. Compounds featuring isolated trigonal Mo_3 units, as in $Zn_2Mn_3O_8$ (6, 7) or $Na_2In_2Mo_5O_{16}$ (8), in which the intercluster distances are 3.235 and 3.1696 Å, respectively, are expected to be insulating due to weak electronic coupling between the neighboring units with respect to both the Mo–Mo direct interactions and the Mo–O–Mo superexchange path, in agreement with the experimental findings. On the other hand, oxides such as KMo_4O_6 (9) and $Mn_{1.5}Mo_4O_{11}$ (10) with infinite linear metal chains formed by joining *trans*-edge-sharing octahedral Mo_6 units spaced only 2.89 Å apart, indeed display metallic behavior along the chain direction. In the case of $LaMo_{8-x}O_{14}$, the intercluster distance of ~3.08 Å is intermediate between those of corresponding metals and insulators, and therefore it was of interest to examine the transport properties of these phases in some detail. We report here the results of the directional electrical transport and magnetic properties of single crystal specimens of $LaMo_{8-x}O_{14}$ prepared by fused salt electrolysis.

EXPERIMENTAL

Good quality crystals of $LaMo_{7.70}O_{14}$ and modulated stoichiometric $LaMo_8O_{14}$ used in the present study were obtained by electrolyzing molten mixtures of sodium molybdate, molybdenum (VI) oxide, and lanthanum oxide at 1050–1080°C in air. For both compounds the best crystals were obtained when the molar ratios Na_2MoO_4:

$MoO_3 : La_2O_3$ were between 3.5 : 3.5 : 1 and 8.5 : 3 : 1, the former ratio being more typical. The total weight of the charge was normally between 30 and 35 gm. A spiral wound from 0.015″ Pt wire served as the cathode while the anode was a 1 cm^2 plate. Currents were typically between 30 and 80 milliamperes. The time of electrolysis varied from a few hours to three days although the shorter times were preferred because of crucible attack. The product adheres to the cathode and is freed of matrix by alternate washes in hot 5% K_2CO_3 and 2 *F* HCl.

The nature of the products depends upon the type of crucible used to contain the melt. If a high density alumina crucible is used (McDanel, 997), the product is $LaMo_{7.70}O_{14}$, free of other reduced co-deposits, and in yields of 0.1–1.5 g depending upon the time of electrolysis. The container is slowly attacked by the melt, as evidenced by the fact that when the electrolysis was carried out for much more than a day, small crystals of corundum were found either adhering tenaciously to the cathode or embedded in the agglomerated product.

If a porcelain crucible (Coors) is used, the product sometimes contains $LaMo_8O_{14}$, usually as part of a mixture in which the major phases are $La_3Mo_4XO_{14}$ (X = Si, Al, Mo), $LaMo_{1+x}Mo_8O_{16}$, and $LaMo_{7.70}O_{14}$. Yields of $LaMo_8O_{14}$ are always poor (e.g., 5–25 mg), but its platelike habit facilitates mechanical separation. These plates are often partially coated with MoO_2, which can be removed by carefully washing with 5 *F* HNO_3 and terminating the reaction immediately after the coating has been removed.

Powder X-ray diffraction patterns were recorded with a Rigaku DMAX-2 diffractometer system using graphite monochromatized Cu radiation. Lattice constants were obtained using a least-squares method. Silicon was used as an internal standard.

The morphology of the "as grown" crystals was often not suitable for directional physical property measurements and several of these crystals had to be polished on a fine emery paper to define directions for attaching electrical contacts. Stereographic projections of the crystals were obtained optically using a two-circle goniometer and the angular information between several faces of the crystals was used to define the direction of the property measurement.

Low temperature electrical resistivity measurements were carried out in a standard four-probe configuration with a Displex cryostat (APD cryogenics, DE-202) in the temperature range 15–300 K. Typical size of the crystals used for resistivity measurements were ~0.5 × 0.9 × 0.5 mm^3. Crystals were first etched in a 5% HF solution at ~70°C for half an hour prior to transport property measurements. Copper leads were then attached to the crystal under a microscope with silver paint. The *I–V* characteristics were monitored at several temperatures in the range 20–300 K to ensure good quality of the contacts during the mesurement. Measurements were carried out on three different crystals from two different sample batches of $LaMO_{7.70}O_{14}$ and one crystal each from two different batches of $LaMo_8O_{14}$. Results within each of the two systems were reproducible to ±20%; i.e., the margin of error in defining the geometric factor of the crystal for the resistivity measurement.

The magnetic susceptibilities measured on batches of randomly oriented single crystals were recorded with a Quantum Design SQUID magnetometer (MPMS) in the temperature range 2–300 K. The data were collected by first cooling the sample to 2 K and then applying a magnetic field of 1000 G. Corrections to the core diamagnetic contributions were applied in the determination of the magnetic susceptibility. Several different samples of the two phase types were measured and the results for each were found to be reproducible within experimental error.

RESULTS AND DISCUSSION

Structure and Composition

$LaMo_{7.70}O_{14}$ and the average structure of $LaMo_8O_{14}$ can be described in terms of the orthorhombic space group *C2ca* (standard setting *Aba2*). In selecting crystals for this study we relied primarily on the characteristic crystal habits of the two phases; oblique thick tablets in the case of $LaMo_{7.70}O_{14}$ and thin six-sided plates in the case of $LaMo_8O_{14}$. However, the X-ray powder diffraction pattern of various samples from which suitable crystals were selected were useful in confirming our choice. Table 1 shows that although the lattice constants are similar for both forms, reproducible differences are observed. In particular, *a* is about 0.04 Å larger for $LaMo_{7.70}O_{14}$ while *b* and *c* are 0.01–0.02 Å smaller as compared to those found for $LaMo_8O_{14}$. In addition, the patterns of $LaMo_{7.70}O_{14}$

TABLE 1
Lattice Parameters of the Samples Used in This Study

Sample	*a*, Å	*b*, Å	*c*, Å
	$LaMo_8O_{14}$		
V-104*	11.129(1)	10.000(1)	9.218(1)
X-77-2A	11.139(1)	10.009(1)	9.219(1)
XI-20-3A	11.138(1)	10.011(1)	9.217(1)
XI-26-3A	11.148(1)	10.005(1)	9.214(1)
	$LaMo_{7.70}O_{14}$		
IX-64-2	11.170(1)	9.991(1)	9.203(1)
EBJ-102	11.173(1)	9.994(1)	9.205(1)
X-51-11	11.174(1)	9.992(1)	9.199(2)
IX-64-2A	11.167(2)	9.989(1)	9.201(1)
X-32-4	11.172(1)	9.990(1)	9.201(1)
EBJ-68-2	11.172(2)	9.990(1)	9.200(1)

show no peaks in the 21°–22° 2θ region, while the $11\bar{2}1$ reflection is clearly evident in the modulated form, as can be seen in Figs. 4a and 4b. The noticeable differences in the relative intensities of the 112 peak at 22.7° are also typical. The small variations in lattice constant are for the most part within the usual limits of reproducibility for these phases. However, the differences could result from small differences in stoichiometry or from intergrowths or stacking faults. Complex intergrowths of modulated and nonmodulated $LaMo_8O_{14}$ have been observed previously (3).

The lattice constant variations might also result from the incorporation of impurities originally present in the starting materials or abstracted from the crucible. Gougeon (5) has recently found that Ti, V, and Cr can substitute for a portion of the Mo in the face-capping sites and it is possible that the electrolysis could concentrate what might be very small amounts of impurities in the melt into quite significant amounts in the cathode product. However, qualitative analysis of our samples at other laboratories by a combination of X-ray fluorescence and electron microprobe analysis shows that no major impurity was consistently present, other than Pt, which were found at levels estimated to be less than 0.5% and believed to be a residual on the crystals from the cathode wires (11–13). In one sample of $LaMo_{7.70}O_{14}$, Al was found at a level of nearly 1%, but it was not detected in two other samples and thus was believed to be in the form of corundum formed as a result of reaction of the melt with the crucible. The quoted stoichiometries were the result of single crystal x-ray diffraction studies (1, 3). The result for $LaMo_{7.70}O_{14}$ has been confirmed independently (14).

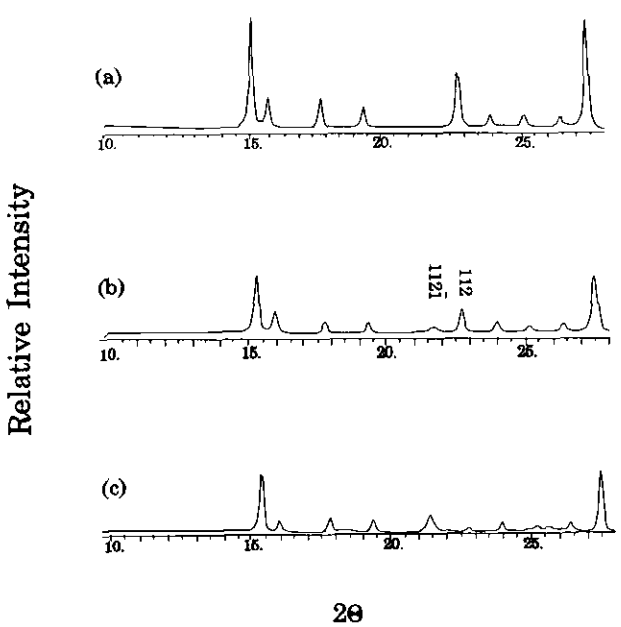

FIG. 4. Partial X-ray powder diffraction patterns of (a) $LaMo_{7.70}O_{14}$, (b) modulated $LaMo_8O_{14}$, (c) $LaMo_8O_{14}$ prepared by a solid state reaction at 1550°C.

Although we believe that the phases prepared in this study are essentially pure lanthanum molybdenum oxides, it is clear that synthesis conditions play a major role in determining what phase is formed. As mentioned previously, a solid state reaction in evacuated, sealed Mo tubes at 1550°C produces $LaMo_8O_{14}$ with a doubled b axis. The material formed in this fashion also appears to have a limited range of nonstoichiometry (14). The diagnostic feature of the X-ray powder diffraction of this form of $LaMo_8O_{14}$ is the presence of a strong peak at approximately 21.4° 2θ and the almost complete absence of a peak at 22.7°, as shown in Fig. 4c. While we find no direct evidence for the formation of this phase by fused salt electrolysis, we have occasionally noted the formation of a definite shoulder on the $11\bar{2}1$ reflection at 21.4°–21.5° 2θ of our $LaMo_8O_{14}$ samples, which could be taken as evidence for the presence of some sort of intergrowth phase. In this respect, it might also be pointed out that an asymmetric broadening of the satellite reflections was a common feature noted in the original single crystal study of modulated $LaMo_8O_{14}$.

Electrical and Magnetic Properties

1. $LaMo_{7.70}O_{14}$. The room temperature resistivities (ρ_{RT}) of $LaMo_{7.70}O_{14}$ measured in the *ab* plane and along the crystallographic *c*-axis are $\sim 5 \times 10^{-3}$ ohm · cm and 2×10^{-2} ohm · cm, respectively. The electrical resistivities as a function of temperature for both directions are shown in Figs. 5 and 6, respectively. As can be seen, particularly from the log(ρ) vs $1/T$ plots (shown in the inset), the behavior of the resistivity as a function of temperature is complex, although in both directions semiconducting behavior was observed down to 15 K.

The thermal activation energy (E_a) values observed are 0.06(1), 0.02(2), and 0.009(6) eV, corresponding to the temperature intervals 200–280 K, 45–105 K, and 16–23 K, respectively, for the measurements in the *ab* plane. The anomalously small E_a value observed in the *ab*-plane (*ca* 0.009 eV) at low temperatures could be attributed to extrinsic effects. The estimated E_a values for the *c*-axis measurements are 0.07(1), 0.3(1), and 0.02(1) eV in the temperature intervals 180–300 K, 85–116 K and 22–37 K, respectively. Although the E_a values in both directions are comparable in the high temperature regime, the E_a for *c* axis measurement at low temperatures is higher than that in the *ab* plane.

The molar magnetic susceptibility of a batch of randomly oriented single crystals of $LaMo_{7.70}O_{14}$ as a function of temperature is shown in Fig. 7. In the temperature range 100–390 K, the increase in the susceptibility is marginal.

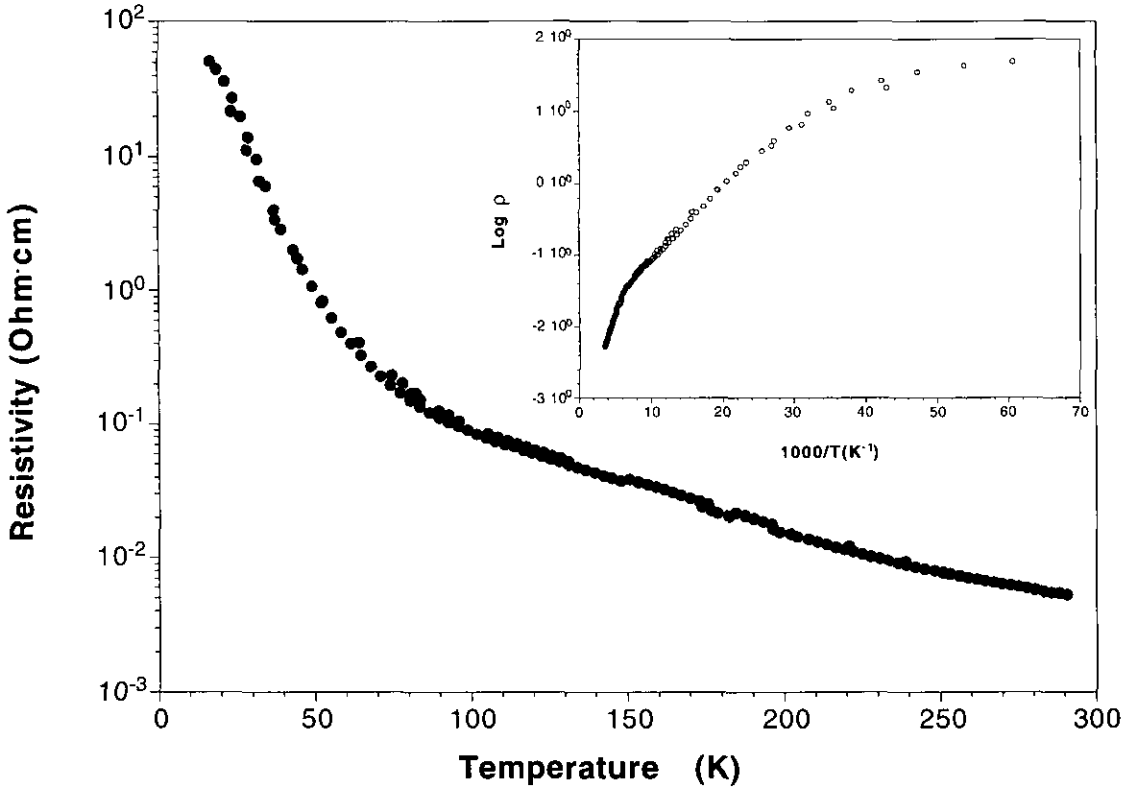

FIG. 5. Temperature dependent electrical resistivity of $LaMo_{7.70}O_{14}$ in the *ab*-plane. Inset shows the Arrhenius plot.

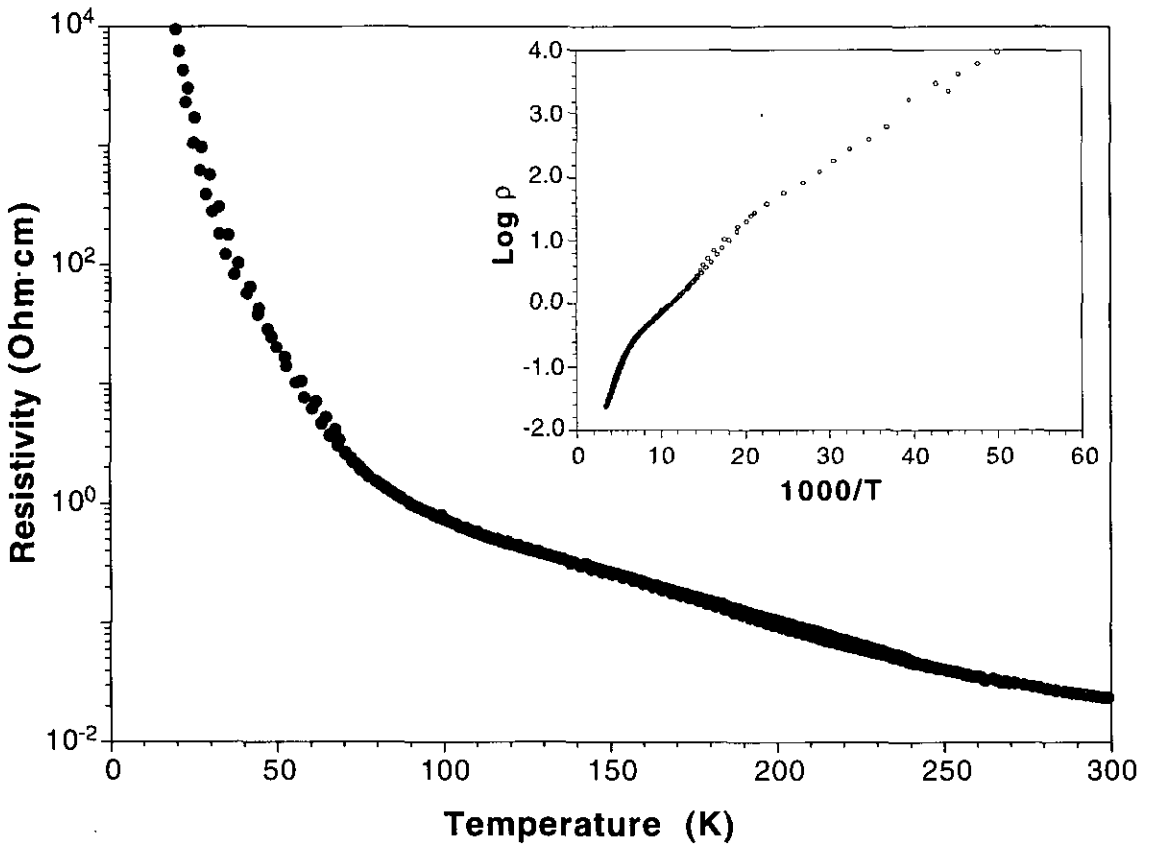

FIG. 6. Temperature variation of the electrical resistivity of $LaMo_{7.70}O_{14}$ measured along the crystallographic *c*-axis. Inset shows the Arrhenius plot.

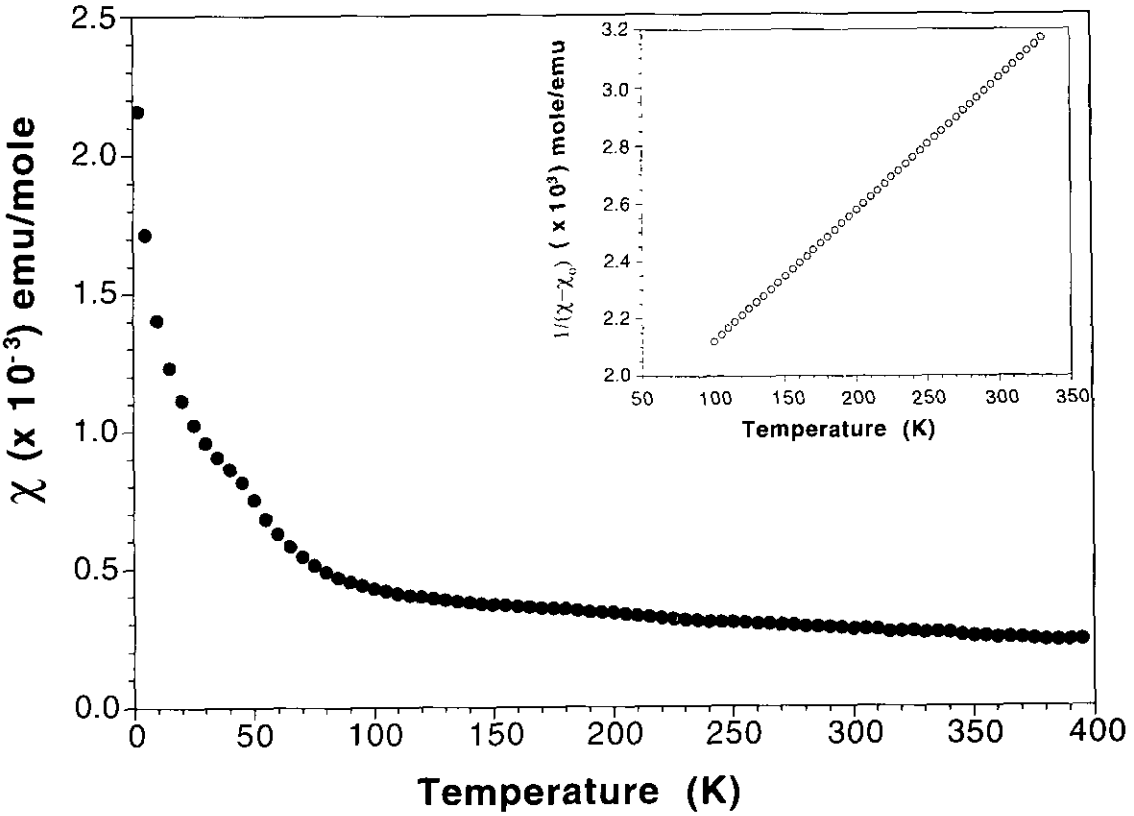

FIG. 7. Variation of the molar magnetic susceptibility as a function of temperature measured on a batch of randomly oriented single crystals of $LaMo_{7.70}O_{14}$. Inset shows the variation of inverse susceptibility, corrected for temperature independent contributions, as a function of temperature.

Below 100 K, however, the susceptibility increases rapidly, with an anomalous kink at ~60 K presumably due to the antiferromagnetic ordering of the adsorbed oxygen (15).

The susceptibility data in the range 100–390 K were fitted to a modified Curie–Weiss relation, $\chi = \chi_0 + C/(T - \theta)$. Here χ_0, C and θ refer to temperature independent susceptibility, the Curie constant, and the Weiss temperature, respectively. A nonlinear least-squares fitting of the observed data yielded $\chi_0 = -5.10 \times 10^{-5}$ emu/mole, $C = 0.219$ emu · K/mole, and $\theta = -364$ K with a root mean squared deviation of ±0.0096. A plot of $1/(\chi - \chi_0)$ as a function of temperature is nearly linear (see inset of Fig. 7), confirming the validity of the above relation. The effective magnetic moment in the range 100–390 K is 1.32 μ_B, which is considerably smaller than the expected value of 1.73 μ_B based on spin-only contributions of 4*d* electrons. These results will be discussed in more detail subsequently.

II. $LaMo_8O_{14}$. The temperature dependence of the electrical resistivity measured with the current applied parallel to the *ab* plane of $LaMo_8O_{14}$ is presented in Fig. 8. The room-temperature resistivity of $LaMo_8O_{14}$ is $\rho_{300K} = 4.4 \times 10^{-2}$ ohm · cm; the resistivity increases with decreasing temperature, indicating semiconducting behavior.

The E_a estimated from the plots of log ρ vs $1000/T$ (shown in the inset of Fig. 8) showed a significant decrease in the vicinity of ~ 130 K. The E_a values in the temperature intervals 200–300 K are 0.071(10) eV and 0.027(10) eV, respectively. The resistivity perpendicular to the *ab*-plane could not be measured due to the small dimensions of the crystal.

The molar magnetic susceptibility corrected for the core-diamagnetic contributions of the constituent ions in $LaMo_8O_{14}$ as a function of temperature is shown in Fig. 9. The susceptibility is temperature-independent and negative in the range 100–300 K, suggesting the absence of localized moments in this compound. The low-temperature upturn seen in the susceptibility may be attributed to the presence of magnetic impurities commonly associated with the rare earth ions.

The electrical and magnetic properties of $LaMo_8O_{14}$ and $LaMo_{7.70}O_{14}$ show significant differences in their tempera-

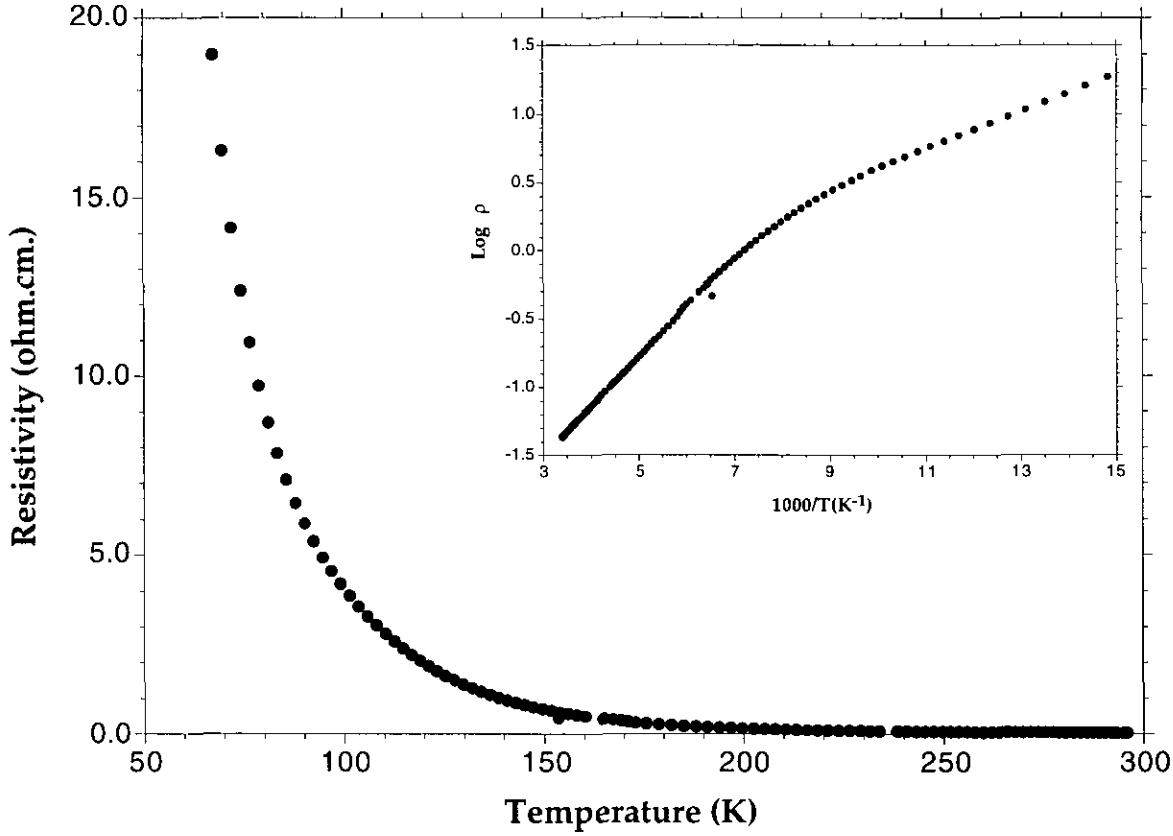

FIG. 8. Electrical resistivity of $LaMo_8O_{14}$ as a function of temperature in the *ab*-plane.

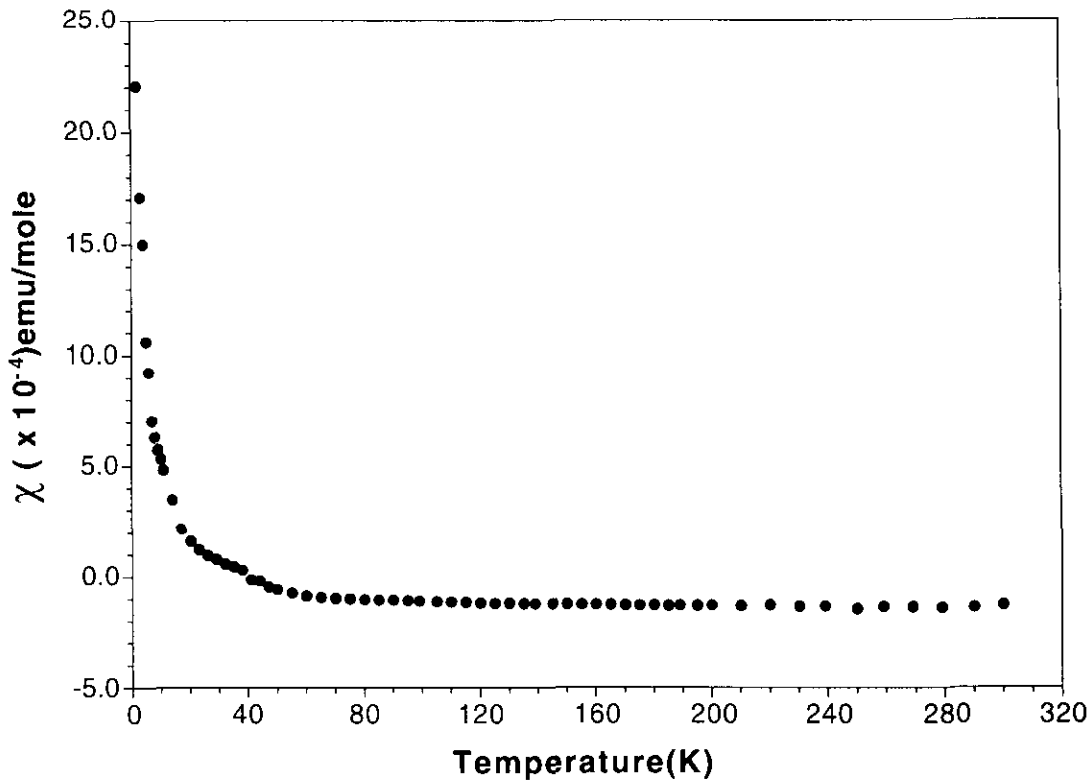

FIG. 9. Molar magnetic susceptibility of $LaMo_8O_{14}$ measured on a batch of randomly oriented single crystals as a function of temperature.

ture dependence. Furthermore, both compounds showed pronounced decreases in the thermal activation energies for electrical conduction at low temperatures, although semiconducting behavior was observed in both compounds.

The markedly different ρ_{RT} values in the *ab* plane and along the *c* axis observed for $LaMo_{7.70}O_{14}$ are indicative of quasi-low-dimensional behavior. The anisotropic factor ρ_{aniso}, defined as the ratio ρ_c/ρ_{ab}, also showed a marked temperature dependence. For example, the value of ρ_{aniso} increased from 4 at room temperature to 264 at ~20 K, suggesting extensive localization of carriers along the *c* axis as compared to the *ab* plane. The preferential localization of carriers along the *c* axis may be related to the asymmetric distribution of Mo–O–Mo intraslab connections. The short ones vary between 1.99 and 2.04 Å, while the long ones are between 2.04 and 2.14 Å. Further, these bonds are not linear. This factor coupled with what appear to be rather long bond distances reduces the likelihood of significant Mo–O–Mo π overlap necessary for metallic conduction parallel to the *c* axis.

The absence of metallic conduction in both compounds may be attributed to an unfavorably long intercluster separation (~3.08 Å) which would result in localization of carriers. Further, the configurational disorder associated with the Mo_8 clusters in $LaMo_8O_{14}$ and the nonstoichiometry of the Mo_8 clusters in $LaMo_{7.70}O_{14}$, significantly reduce the effective overlap of 4*d* orbitals necessary for the formation of wide conduction bands thus accounting for the semiconducting property. The relatively higher resistivity of $LaMo_8O_{14}$ ($\rho_{RT} = 4 \times 10^{-2}$ ohm · cm) compared to $LaMo_{7.70}O_{14}$ ($\rho_{RT} = 5 \times 10^{-3}$ ohm · cm) underscores the importance of configurational disorder associated with the Mo_8 clusters in the former compound.

The magnetic susceptibilities of $LaMo_8O_{14}$ and $LaMo_{7.70}O_{14}$, measured as a function of temperature, illustrate contrasting behavior. The effective magnetic moment of 1.32 μ_B observed for $LaMo_{7.70}O_{14}$ indicates the presence of localized electrons. However, the reason for the diamagnetic behavior observed for the stoichiometric compound $LaMo_8O_{14}$ is not clear at present.

Detailed electronic band structure calculations would be helpful in probing these differences. Preliminary calculations based on the *cis*-only structure of $NdMo_8O_{14}$ have been carried out by Martin and Canadell (16) and should be applicable to $LaMo_{7.70}O_{14}$. Their results show 11 low-lying *d* bands below the Fermi level that could accommodate 22 electrons. The 21.2 electrons per cluster of $LaMo_{7.70}O_{14}$ would only partially fill the upper most band leading to a net of 0.8 unpaired electrons per cluster, in line with the observed moment of 1.32 μ_B. Since the bands are narrow the compound should be semiconducting and exhibit localized behavior.

While their band calculations are not applicable to the modulated form of $LaMo_8O_{14}$, they also derived qualitative molecular orbital energy diagrams for mono- and bi-faced capped octahedral clusters which, when used with existing models for M_6 octahedral clusters, might be useful for predicting the magnetic moments in both compounds. However, electron fillings based upon their models predict that $LaMo_{7.70}O_{14}$ would have a very weak paramagnetism corresponding to 0.1–0.2 unpaired spins per formula unit while $LaMo_8O_{14}$ would have about 0.4 unpaired spins per formula unit, neither of which predictions is consistent with our findings. The failure of the model may be due to a variety of factors including distortion of the clusters from ideal symmetry, modulation effects in the stoichiometric compound, as well as nonstoichiometry and intergrowth effects more complex than those studied previously.

ACKNOWLEDGMENT

We thank Professor Patrick Gougeon for sending us samples of his solid state preparations of $LaMo_8O_{14}$ for our X-ray powder diffraction study. We also thank Professor Phillipe Labbé for the goniometric studies used to define the crystal orientation. This work was supported by the National Science Foundation under Solid State Chemistry Grant DMR-90-19301.

REFERENCES

1. H. Leligny, M. Ledesert, P. Labbé, B. Raveau, and W. H. McCarroll, *J. Solid State Chem.* **87,** 35 (1990).
2. P. Gougeon and R. E. McCarley, *Acta Crystallogr. Sect. C* **47,** 241 (1991).
3. H. Leligny, P. Labbé, M. Ledesert, M. Hervieu, B. Raveau, and W. H. McCarroll, *Acta Crystallogr. Sect. B* **49,** 444 (1993).
4. G. Kerihuel and P. Gougeon, submitted for publication.
5. P. Gougeon, private communication.
6. W. H. McCarroll, L. Katz and R. Ward, *J. Am. Chem. Soc.* **79,** 5410 (1957).
7. G. B. Ansell and L. Katz, *Acta Crystallogr.* **21,** 482 (1966).
8. B. Collins, S. Fine, J. Potenza, P. P. Tsai, and M. Greenblatt, *Inorg. Chem.* **28,** 2444 (1989).
9. K. V. Ramanujachary, M. Greenblatt, E. B. Jones, and W. H. McCarroll, *J. Solid State Chem.* **102,** 69 (1993).
10. R. E. McCarley, K. H. Lii, P. A. Edwards, and L. F. Brough, *J. Solid State Chem.* **57,** 17 (1985).
11. J. Chardon, Université de Caen.
12. L. Moore, Rheox Laboratories, Hightstown, NJ.
13. E. A. C. Laboratories, Tallahassee, FL.
14. P. Gougeon, private communication.
15. "Quantum Design Technical Advisory MPMS No. 8," Quantum Design, 1990.
16. J. D. Martín and E. Canadell, Abstr. No. 359, Inorg. Div., 204th Natl. Meeting, Amer. Chem. Soc., Washington, DC, 1992.